JCTC Journal of Chemical Theory and Computation

Article

pubs.acs.org/JCTC

Effects of Dispersion in Density Functional Based Quantum Mechanical/Molecular Mechanical Calculations on Cytochrome P450 Catalyzed Reactions

Richard Lonsdale, Jeremy N. Harvey,* and Adrian J. Mulholland*

Centre for Computational Chemistry, School of Chemistry, University of Bristol, Cantock's Close, Bristol BS8 1TS, U.K.

Supporting Information

ABSTRACT: Density functional theory (DFT) based quantum mechanical/molecular mechanical (QM/MM) calculations have provided valuable insight into the reactivity of the cytochrome P450 family of enzymes (P450s). A failure of commonly used DFT methods, such as B3LYP, is the neglect of dispersion interactions. An empirical dispersion correction has been shown to improve the accuracy of gas phase DFT calculations of P450s. The current work examines the effect of the dispersion correction in QM/MM calculations on P450s. The hydrogen abstraction from camphor, and hydrogen abstraction and C−O addition of cyclohexene and propene by $P450_{cam}$ have been modeled, along with the addition of benzene to Compound I in CYP2C9, at the B3LYP-D2/CHARMM27 level of theory. Single point energy calculations were also performed at the B3LYP-D3//B3LYP-D2/CHARMM27 level. The dispersion corrections lower activation energy barriers significantly (by ∼5 kcal/mol), as seen for gas phase calculations, but has a small effect on optimized geometries.These effects are likely to be important in modeling reactions catalyzed by other enzymes also. Given the low computational cost of including such dispersion corrections, we recommend doing so in all B3LYP based QM/MM calculations.

INTRODUCTION

Density functional theory (DFT) based quantum mechanics (QM) and quantum mechanics/molecular mechanics (QM/MM) studies have been used extensively to study the factors that are involved in the reactivity of enzymes, for example the numerous studies of the cytochromes P450 (P450s).[1−25] P450s are of great interest to the pharmaceutical industry, as they are responsible for the metabolism of a significant proportion of ingested foreign compounds, including drugs.[24,26] Modeling the reactions of drugs in P450s may help to rationalize and predict the formation of toxic products formed during the metabolism of drug candidates, and highlight potential adverse drug reactions at an early stage in the drug discovery process.[24]

The intermediate responsible for performing oxidation reactions in P450s is an iron-oxo porphyrin species (Compound I - Cpd I), and hence modeling the chemical transformations that take place at the active site in P450s requires a QM method that can reliably obtain the correct electronic configuration of this complex moiety. The electrostatic and steric effects of the protein environment have been shown to have a significant effect on the calculated electronic structure of Cpd I.[1,5,23] QM/MM calculations of Cpd I provide a model that is more representative of the species in the enzyme than in gas phase QM-only calculations of an active site model, because here the effects of the protein environment are included explicitly.[1,5,23] In QM-only studies the enzyme environment is either ignored completely or treated in an approximate manner, for example by the inclusion of a continuum solvation model and/or N−H groups hydrogen bonding to the thiolate (or methyl mercaptide) sulfur that is used to represent the heme-bound cysteine.[27,28] A recent QM/MM study of the metabolism of dextromethorphan by CYP2D6 highlighted the effect that the protein surrounding the active site can have in controlling the regioselectivity of oxidation.[22] In that study, B3LYP barriers calculated in the gas-phase suggested that both *O*-demethylation and aromatic hydroxylation might occur, despite an experimental preference for *O*-demethylation. However, a strong preference for *O*-demethylation was predicted in B3LYP/CHARMM27 QM/MM calculations using a large protein model because in this example, like for many drugs, the amino acid residues surrounding the enzyme active-site affect the accessibility of the potential metabolism sites to Cpd I. Specifically for dextromethorphan in CYP2D6, this was due to subtle effects particularly disfavoring formation of the transition state for aromatic hydroxylation.

For enzyme systems that do not contain a transition metal containing cofactor, highly accurate ab initio QM methods, such as coupled-cluster and those based on Møller−Plesset perturbation theory (e.g., MP2), can be used in QM/MM calculations.[29] Use of these methods is not yet routine, though, and may even not be possible for open-shell systems with significant static correlation effects such as enzymes with transition metal cofactors in the active site. Hence DFT methods remain the most appropriate for use in QM/MM studies of many metalloenzymes. B3LYP is the most commonly used functional for modeling P450s, despite some reported inaccuracies for other systems, because it reliably predicts the ground state electronic structure of many of the intermediates in the catalytic cycle of P450s at reasonable computational expense.[30] One problem that has been observed in both B3LYP and B3LYP/MM studies of P450s is that the potential energy barriers for reaction are often calculated to be higher than those

Received: April 27, 2012
Published: August 21, 2012

suggested from experimental studies, an example being the hydroxylation of camphor by $P450_{cam}$.[12] It is worth noting that B3LYP also overestimates barriers for some nonmetalloenzymes, such as citrate synthase.[31] However, B3LYP has been found to underestimate activation energy barriers for some other enzyme reactions.[32]

Many DFT functionals (including B3LYP) have several well-known limitations, including the self-interaction error and medium- and long-range correlation errors.[33] The missing dispersion interaction in B3LYP is believed to contribute to the overestimation of activation barriers for P450 enzymes.[34] Several approaches have been designed to overcome the neglect of dispersion, and have shown encouraging results;[35,36] inclusion of an empirical R^{-6} correction to the DFT energy (e.g., the "D2" and "D3" corrections developed by Grimme[37,38]), or empirical fitting of density functionals to reproduce dispersion interactions (e.g., the M06 functional developed by Truhlar and co-workers),[39] or by intrinsic inclusion of such interactions in the functional (e.g., Becke's DF07 fuctional[40]). The first of these approaches (i.e., the "D2" correction) is the least computationally expensive method for the systems studied here, and the correction (shown below) has been parametrized for B3LYP, among other functionals.

$$E_{\mathrm{disp}} = -s_6 \sum_{i=1}^{N_{\mathrm{at}}-1} \sum_{j=i+1}^{N_{\mathrm{at}}} \frac{C_6^{ij}}{R_{ij}^6} f_{\mathrm{dmp}}(R_{ij}) \quad (1)$$

$$f_{\mathrm{dmp}}(R_{ij}) = \frac{1}{1 + e^{-d(R_{ij}/R_r - 1)}} \quad (2)$$

The inclusion of the D2 correction[37] in B3LYP QM-only model calculations of P450 catalyzed reactions has been investigated,[34] focusing on the hydrogen-abstraction step in the hydroxylation of camphor, cyclohexene, and propene, together with the carbon−oxygen bond formation step in the epoxidation of cyclohexene and propene. The dispersion energy and its gradient correction were included in geometry optimization, and hence the effect on both the geometries and the energies of key reacting species was investigated. A significant effect was observed, both on the calculated geometries of transition states and encounter complexes and on the relative energies of these species. In the dispersion-corrected calculations (in contrast to the noncorrected calculations) the substrates adopted orientations in which the maximum number of substrate atoms were able to form dispersion interactions with the porphyrin ring. Because dispersion is an attractive force, the effect of this interaction is to decrease the energies of encounter complexes and transition states relative to the reacting species at infinite separation. In the QM-only study, the transition states were lowered in energy to a larger extent than the corresponding encounter complexes, and hence the dispersion correction lowered the activation barriers calculated relative to the complexes for all of the processes studied. Prior to this work, most studies that involved this dispersion correction were limited to application using a single point correction. The study highlighted the importance of including the dispersion correction in geometry optimization, due to the large difference between B3LYP and B3LYP-D2 optimized geometries.

Several QM/MM studies have been performed recently in which a dispersion correction has been applied to the B3LYP functional.[41,42] For example, Schyman et al. studied the formation of dopamine in CYP2D6 with B3LYP/CHARMM and observed a significant lowering of activation energies when these were corrected for dispersion using single point calculations.[42] However, common to most of the reported QM-only studies in which dispersion has been included, the correction was added as a single point energy correction to the barriers, and the effect of adding the dispersion correction on the calculated geometries was not investigated.

Generally, in QM/MM calculations dispersion interactions are included between MM atoms by the Lennard-Jones term used in the calculation of nonbonded interactions. The interaction between QM and MM atoms is also included in the same way. However, for QM/MM calculations in which many popular density functionals are used, there is no dispersion interaction included between the QM atoms. In the present paper, we shall describe work in which an empirical dispersion correction[37] is included in B3LYP-based QM/MM calculations of some important P450 model reactions, namely, the hydroxylation of camphor, cyclohexene, and propene by CYP101 from *Pseudomonas putida* ($P450_{cam}$), the epoxidation of cyclohexene and propene by $P450_{cam}$, and the hydroxylation of benzene by CYP2C9. These systems provide an excellent test for the effect of dispersion on QM/MM calculations in cytochrome P450 enzymes. In this work, as with our QM-only study,[34] we apply the dispersion correction to both the energies and the gradients and hence are able to investigate the effect that dispersion has on calculated geometries. We show that for the calculation of energy barriers, a similar trend is observed to that seen in our previous QM-only study,[34] but a smaller effect is observed for optimized geometries.

Here, as with our previous work[12,14,20,22] (and work by others[4,11,19,41,43]), we aim to calculate activation energy barriers for a specific step in the P450 catalytic cycle: the oxidation of substrate by the Cpd I intermediate, starting from the Cpd I - substrate complex. Hence our study addresses the impact of including dispersion effects within the QM/MM calculations on the rate constant for this step (in a simple Michaelis−Menten framework, k_{cat}). As found in our QM study [34], including dispersion also changes the energy of the Cpd I -substrate complex relative to separated reactants, so it is likely that calculations of the substrate binding constant, K_M, would also yield rather different results with and without including dispersion. However, calculation of K_M in a QM/MM framework is very challenging and is not addressed here. Also, our calculations address the activation energy for the oxidative step, rather than the free energy. As might be expected for what is formally a unimolecular step, it is generally observed, from both experiment[44] and computation,[29,32,45] that the activation entropy associated with k_{cat} is small (~ 0.5 kcal/mol for H-atom abstraction in $P450_{cam}$[45]), so that the free energy of activation should be similar to the energy of activation computed here. We note that in previous work on oxidation of a variety of substrates in phenol hydroxylase[46] and para-hydroxybenzoate hydroxylase,[47] calculated $\Delta E^{\ddagger}$ values for some enzyme-catalyzed reactions have been shown to correlate very well with the logarithm of experimental k_{cat} values, as expected if entropic effects are small for k_{cat}.

COMPUTATIONAL DETAILS

Several P450 catalyzed reactions were modeled using dispersion-corrected (B3LYP-D2)QM/MM and are reported here. The QM subsystems are shown in Figure 1 and are composed of a Cpd I model consisting of an iron-oxo-porphine bound to a methyl mercaptide group ($^{-}SCH_3$), together with

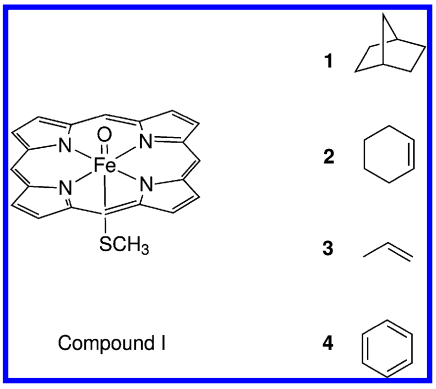

Figure 1. QM models used here in the QM/MM calculations of P450 catalyzed oxidation of (**1**) camphor, (**2**) cyclohexene, (**3**) propene, and (**4**) benzene. The QM model for Compound I is shown on the left and the respective substrates on the right.

substrate. This QM/MM partitioning scheme has been tested and used previously.[5,12,14,20] The remainder of the protein and solvent were treated at the MM level. The aliphatic hydroxylation reactions of camphor (**1**), cyclohexene (**2**), and propene (**3**) by $P450_{cam}$ were modeled. The epoxidation of **2** and **3** by $P450_{cam}$ was also modeled. The aromatic hydroxylation of benzene (**4**) was modeled in the CYP2C9 isoform with both the side- and face-on orientations of benzene relative to the plane of the heme ring, as shown in Scheme 1.

Scheme 1. Side-on and Face-on Mechanisms for Addition of Benzene to Cpd I[48]

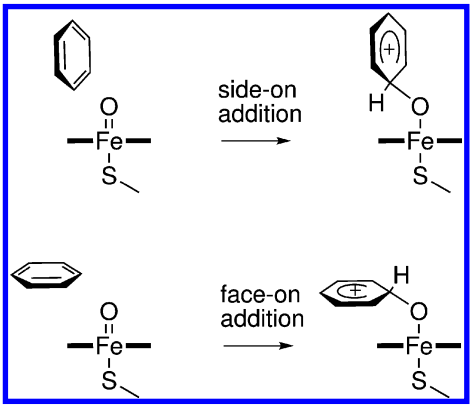

The side- and face-on additions of benzene to Cpd I have been modeled with B3LYP/MM previously,[14] however, it is possible that inclusion of a dispersion correction may favor one orientation over the other.

All calculations were performed at the QM/MM level using the QoMMMa program,[49] in which the QM calculations are performed in Jaguar[50] using the B3LYP density functional,[51−54] with the point charges from the MM region included in the QM Hamiltonian. For geometry optimization, the Los Alamos effective core potential (LACVP)[55] was used for Fe and the 6-31G(d) basis set for all other atoms.[56] Single point energies were calculated for all optimized reactant complex and transition state geometries at the LACV3P,[57] 6-311++G(d,p) level;[58−61] the energies calculated at this level are those presented here. The MM part of all QM/MM calculations was performed in Tinker,[62] using the CHARMM27 forcefield.[63] To satisfy the valence of the QM atoms at the QM/MM boundary, link atoms (modeled as hydrogen atoms) were used.[64] The charges of the MM atoms at the QM/MM boundary were set to zero to avoid unphysical interactions with the link atoms, and the residual charge was shifted onto adjacent atoms to maintain the same net charge.[65]

For all calculations denoted B3LYP-D2, an empirical dispersion correction[37] (see eqs 1 and 2) was calculated for the QM atoms (not link atoms) at each QM step, together with the first derivative, and these were subsequently added to the respective QM energy and gradient. All calculations were also performed in the absence of the dispersion correction; these are denoted B3LYP. Additionally, single point energies inclusive of dispersion were calculated for the B3LYP optimized geometries and are denoted B3LYP-D2//B3LYP.

Dispersion interactions are included in the QM/MM interaction energy, by using standard Lennard-Jones parameters for the QM atoms, as used in the MM force field. The choice of these parameters can be important for QM/MM interactions,[66] but the focus here is on studying the effects of including dispersion within the QM region itself.

The dispersion energy correction was also calculated for several QM geometries using the DFT-D3 method.[38] These calculations were performed using the QM geometries optimized at the B3LYP-D2/CHARMM27 level. The DFTD3 program was used to calculate these energies.[67]

For calculations of $P450_{cam}$, the 1DZ9 crystal structure solved by Schlichting et al. was used.[68] For CYP2C9, the 1OG2 crystal structure, solved by Williams et al. was used.[69] Starting structures were obtained from stochastic boundary molecular dynamics simulations, performed with the CHARMM program, version 30b2,[70] with stochastic boundary conditions. Similar procedures have been applied successfully in previous simulations of P450s and other enzymes.[5,12,14,20,23,25] Further details of the setup procedure for these simulations are included in the Supporting Information.

The mechanistic features of the reactions modeled in this study have been explored previously[12,14,20,48,71,72] and are only briefly outlined here. Aliphatic hydroxylation by Cpd I proceeds via the "rebound" mechanism in which the first (and rate-limiting) step is the abstraction of a hydrogen atom from the substrate (Scheme 2).[73,74] This step was modeled here by

Scheme 2. Hydrogen Abstraction from Alkane R-H by Cpd I[a]

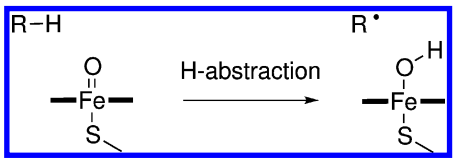

[a]The bold lines flanking the Fe represent the porphyrin ring.

defining a reaction coordinate as the distance between the hydrogen atom undergoing abstraction and the Cpd I ferryl oxygen atom. This reaction coordinate has been used previously and was shown to reliably model this reaction step.[4,12] The geometry was optimized using QM/MM at specific intervals along the reaction coordinate, leading sequentially from the reactant complex to the radical intermediate via the transition state. The reaction coordinate was restrained using an harmonic potential with a force constant of 1000 kcal mol^{-1} $Å^{-2}$. The coordinate was decreased in steps of 0.2 Å, with the exception of the region close to the transition state, where smaller steps of 0.1 Å were used. The

activation potential energy barrier, $\Delta E^{\ddagger}$, was calculated as the difference in energy between the reactant complex and transition state species.

The mechanism for alkene epoxidation by Cpd I involves initial C−O bond formation (rate-limiting) between a substrate alkene carbon atom and the Cpd I oxygen atom, to form a radical intermediate (Scheme 3).[20,71] This process was modeled using a similar procedure to that used to model aliphatic hydroxylation, with the difference that the C−O bond distance was used as the reaction coordinate in this case.

Scheme 3. C−O Bond Formation Step during the Oxidation of Alkene R-CH_2=CH_2 by Cpd I[a]

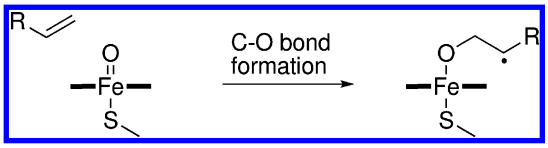

[a]The bold lines flanking the Fe represent the porphyrin ring.

The consensus mechanism for aromatic hydroxylation by Cpd I is the addition-rearrangement mechanism, where an initial σ-intermediate is formed between an aromatic carbon atom and the Cpd I oxygen (1).[48] This intermediate can undergo several different rearrangement processes to form epoxide, ketone, and phenol products.[14,48] As the formation of the σ-intermediate is likely to be rate-limiting,[14,48] this step alone is considered in the current work. It was modeled in an analogous way to the other model systems, in this case the C−O bond distance was used as the reaction coordinate. The same harmonic restraint was used as for hydrogen abstraction, as detailed above.

Cpd I has two electronic states that lie close in energy, due to the two different coupling patterns that can occur between the three unpaired electrons: a doublet and quartet. Both of these states have been identified as likely to contribute to the reactivity of this species,[75] hence both were modeled here for camphor and benzene hydroxylation. Both spin states were found to give similar calculated energy barriers, as found in our QM-only study,[34] so for alkene oxidation by $P450_{cam}$ only the quartet state of Cpd I was studied here.

RESULTS AND DISCUSSION

The addition of the dispersion correction[37] to the QM/MM calculation does not add any significant amount of computational expense to each QM/MM energy (and gradient) evaluation. Also, on average, the dispersion corrected QM/MM calculations achieved convergence in the same number of geometry optimization steps as those performed in the absence of the correction. The electronic structure of Cpd I was checked in all calculations, to verify convergence to the correct wave function.[25] The electronic structure of Cpd I did not differ between the B3LYP-D2 and B3LYP calculations, as shown by inspection of Mulliken charges and spin densities (details in the Supporting Information). This shows that the changes in structure associated with optimization using the dispersion correction are not large enough to cause major changes in electronic structure.

The results are presented in two parts. First, the dispersion corrected activation barriers (from large basis set, single point calculations) for the oxidation processes studied here are presented. Second, the optimized structures of the reactant complexes and transition states calculated with dispersion corrected QM/MM are described. This allows separate consideration of the effects on energies and structures. Throughout, the results are compared with those from calculations on the same systems with the same calculations performed without the dispersion correction.

Effect of Dispersion on Activation Energy Barriers. In our previous QM-only study on small models of CYP reactions,[25] the activation energy barriers for the hydroxylation of camphor, and the hydroxylation and epoxidation of cyclohexene and propene were found to be lowered by between 1 and 6 kcal/mol upon the addition of the dispersion correction, when the dispersion interaction was included in the geometry optimization.[34] This is because the dispersion correction lowered the energies (relative to separate reactants) of the transition states to a greater extent than those of the reactant complexes. The effect of dispersion on barriers for aromatic hydroxylation has not been reported previously. The activation barriers for all reactions in the $P450_{cam}$ and CYP2C9 isoforms studied in this work are discussed below.

Hydroxylation of Camphor by $P450_{cam}$. The hydroxylation of camphor by $P450_{cam}$ to form 5-exohydroxycamphor has been investigated previously by several groups using QM/MM methods.[9,11−13] The hydrogen abstraction step was found in these studies to have an energy barrier in the range of 17 to 20 kcal/mol, depending on the choice of basis set and QM system size.

The calculated barriers for abstraction of the 5-*exo* hydrogen atom from camphor by the Cpd I ferryl oxygen in $P450_{cam}$ are displayed in Table 1. A zero point energy correction has not been calculated here but was found previously to lower the barrier by approximately 5 kcal/mol when calculated in the gas phase.[34] The B3LYP barriers are in good agreement with previous QM/MM studies of camphor hydroxylation by $P450_{cam}$.[9,11−13] The addition of the dispersion correction to the QM/MM calculations results in the lowering of the barriers by between 2.3 and 4.8 kcal/mol. As we found in our QM-only study, the inclusion of the dispersion correction in single point energy calculations (B3LYP-D2//B3LYP - i.e. without geometry optimization) has a smaller effect in lowering the barrier compared to calculations performed with the dispersion correction included in the geometry optimization. With zero point energy corrections taken into account, the doublet B3LYP-D2/CHARMM27 barrier is approximately 8.3 kcal/mol, significantly lower than the barrier of 12.1 kcal/mol calculated in the QM-only study.[34] The barriers calculated on the doublet and quartet spin surfaces are very similar, as has

Table 1. Activation Energy Barriers, $\Delta E^{\ddagger}$, [in kcal/mol] for Aliphatic Hydroxylation of Camphor by $P450_{cam}$[a]

B3LYP-D2		B3LYP		B3LYP-D2//B3LYP	
$^2\Delta E^{\ddagger}$	$^4\Delta E^{\ddagger}$	$^2\Delta E^{\ddagger}$	$^4\Delta E^{\ddagger}$	$^2\Delta E^{\ddagger}$	$^4\Delta E^{\ddagger}$
13.3	14.0	18.1	18.3	15.2	16.0

[a]Barriers are calculated with QM/MM with (B3LYP-D2/CHARMM27 - B3LYP-D2) and without dispersion (B3LYP/CHARMM27 - B3LYP). Barriers are also calculated with B3LYP-D2/CHARMM27 at the B3LYP/CHARMM27 geometries (B3LYP-D2//B3LYP). The values presented in this table were calculated on the doublet and quartet spin surfaces (denoted with superscripts 2 and 4, respectively) with the LACV3P (Fe), 6-311++G(d,p) (other atoms) basis set.

dx.doi.org/10.1021/ct300329h | J. Chem. Theory Comput. 2012, 8, 4637−4645

been observed in previous QM and QM/MM studies.[34] The experimental rate constant for abstraction of hydrogen from camphor by $P450_{cam}$ is not known, but an upper limit of 15 kcal/mol for the energy barrier, based on the overall rate of turnover, was suggested previously.[12] The calculated barrier of 8.3 kcal/mol at the B3LYP-D2/CHARMM27 level is well below this upper limit. Given the high reactivity of Cpd I, and experimental elusiveness until very recently,[76] it is not surprising that such a low barrier is calculated for this step. A fuller comparison with experiment would require sampling of multiple substrate and protein conformations[20] and consideration of other steps in the reaction; such a comparison is beyond the scope of the current work where the aim is simply to examine the effects of dispersion.

Hydroxylation of Benzene in CYP2C9. The hydroxylation of benzene (and derivatives) by Cpd I has been modeled previously (in the absence of dispersion effects), both in a QM-only model[48,72] and with QM/MM.[14] The rate-limiting step in this process is the formation of a bond between the Cpd I oxygen and the substrate aromatic carbon atom. Reactions involving two possible orientations of the benzene molecule relative to the heme have been identified in previous work:[48,72] side-on, where the benzene ring is approximately perpendicular to the plane of the heme; and face-on, where the benzene ring is approximately parallel to the plane of the heme (1). In QM-only model calculations of benzene addition, the barrier to electrophilic addition was found to be slightly lower (by 2.3 kcal/mol) for the side-on orientation.[48,72] In the previous QM/MM study of CYP2C9, no significant preference could be detected, suggesting that the protein environment may play a role in modulating the preference for these mechanisms.[14] In the present work, the effect of dispersion on the magnitude of the barrier to addition of benzene to Cpd I in CYP2C9, and the preferred substrate orientation, are explored.

The calculated barriers for addition of benzene to Cpd I are displayed in Table 2. The B3LYP QM/MM barriers are consistent with those calculated previously.[14] Both the B3LYP-D2 and B3LYP-D2//B3LYP barriers are significantly lower than those calculated without dispersion by between 3.0 and 7.0 kcal/mol. This represents a larger effect in lowering the barrier than was observed in the case of camphor (2.3−4.8 kcal/mol, see above). One might expect the effect of dispersion to be smaller for benzene than for camphor, because camphor is a larger substrate and hence a larger dispersion correction is expected. However, the dispersion correction to the barrier is not only affected by the number of atoms in the reactants, but also by the proximity of the reactants at the transition state. If the reactants are closer together at the transition state for aromatic hydroxylation than they are for aliphatic hydroxylation, a larger dispersion correction would be expected for the former. In the QM-only study,[34] the barriers for propene and cyclohexene oxidation were lowered to a greater extent with the addition of dispersion, compared to camphor hydroxylation. Clearly, the effect of dispersion is not simply uniform and depends on both the reactants and the reaction taking place.

Table 2. Activation Energy Barriers, $\Delta E^{\ddagger}$, [in kcal/mol] for Hydroxylation of Benzene by CYP2C9[a]

	B3LYP-D2		B3LYP		B3LYP-D2//B3LYP	
	$^2\Delta E^{\ddagger}$	$^4\Delta E^{\ddagger}$	$^2\Delta E^{\ddagger}$	$^4\Delta E^{\ddagger}$	$^2\Delta E^{\ddagger}$	$^4\Delta E^{\ddagger}$
side-on	13.5	11.9	20.4	20.2	15.5	15.5
face-on	13.9	15.5	18.4	20.3	13.8	17.3

[a]Barriers are calculated with QM/MM with (B3LYP-D2/CHARMM27 - B3LYP-D2) and without dispersion (B3LYP/CHARMM27 - B3LYP). Barriers are also calculated with B3LYP-D2/CHARMM27 at the B3LYP/CHARMM27 geometries (B3LYP-D2//B3LYP). The values presented in this table were calculated on the doublet and quartet spin surfaces (denoted with superscript 2 and 4, respectively) with the LACV3P (Fe), 6-311++G(d,p) (other atoms) basis set.

In the previous QM/MM study of reaction in CYP2C9 (without dispersion),[14] two profiles each were calculated for side-on and face-on addition. It was not possible to identify a preferred orientation from these because the difference in barriers was within the error bars associated with the method. In the present work the B3LYP-D2/CHARMM27 barriers also are roughly the same for side-on and face-on addition in the doublet spin state (13.5 and 13.9 kcal/mol respectively), while for the quartet spin state the barriers suggest a preference for the side-on orientation (11.9 and 15.5 kcal/mol respectively, see Table 2). These differences are still of the same order as the estimated error for these calculations. Our calculations, which do not include sampling of any further conformations compared to our earlier QM/MM study,[20] yield lower reaction barriers, but support its conclusion that side-on and face-on orientations for reaction should be competitive.

Oxidation of Cyclohexene and Propene in $P450_{cam}$. In the previous work,[20] the QM/MM calculated barriers to epoxidation and hydroxylation of cyclohexene and propene in $P450_{cam}$ were found to be highly dependent on the orientation of the substrate relative to Cpd I in the reactant complex and transition state. Several profiles have been recalculated here to investigate the likely link between the orientation of the substrate molecule and the magnitude of the dispersion correction. Four profiles were calculated for the hydroxylation (and three for epoxidation) of cyclohexene by $P450_{cam}$. To reduce computational expense, only the quartet spin state of Cpd I is considered, because the choice of spin state does not have a major effect on the magnitude of the dispersion correction, as doublet and quartet reactivity involves similar structures.[34] The calculated barriers, both with and without dispersion (and for single point corrections calculated for structures optimized without dispersion), are shown in Table 3.

The dispersion correction is clearly not uniform within each set of hydroxylation and epoxidation profiles. This is expected, given that the dispersion correction to the energy barrier will vary depending on the relative orientation of the atoms in both the transition state and reactant complex geometries. As found for the other substrates modeled, the B3LYP-D2 and B3LYP-D2//B3LYP QM/MM barriers are lower than the corresponding barriers calculated in the absence of dispersion (B3LYP). Additionally, the calculated corrections to the B3LYP/CHARMM27 barriers span similar ranges of values for the B3LYP-D2 calculations (4.1−8.3 kcal/mol) and B3LYP-D2//B3LYP calculations (4.3−6.9 kcal/mol). The effect of dispersion on the hydroxylation barriers is similar to that on the epoxidation barriers. This is slightly surprising, because for epoxidation of cyclohexene (where the C=C π system must approach the heme) one might expect the substrate to approach Cpd I slightly more closely to react, compared with the hydroxylation reaction (hydrogen atom abstraction). This would result in a greater dispersion correction for that TS and hence greater lowering of the activation barrier compared to the

Table 3. Activation Energy Barriers, $\Delta E^{\ddagger}$, [in kcal/mol] for Hydroxylation and Epoxidation of Cyclohexene by $P450_{cam}$[a]

		$\Delta E^{\ddagger}$		
	profile	B3LYP-D2	B3LYP	B3LYP-D2//B3LYP
hydroxylation	1	9.6	17.5	14.0
	2	11.4	16.5	13.5
	3	10.4	14.5	10.2
	4	14.1	21.9	17.6
epoxidation	1	14.8	21.4	15.1
	2	12.3	19.3	14.1
	3	10.3	18.6	13.7

[a]Barriers are calculated with QM/MM with (B3LYP-D2/CHARMM27 - B3LYP-D2) and without dispersion (B3LYP/CHARMM27 - B3LYP). Barriers are also calculated with B3LYP-D2/CHARMM27 at the B3LYP/CHARMM27 geometries (B3LYP-D2//B3LYP). The values presented in this table were calculated on the quartet spin surface with the LACV3P (Fe), 6-311++G(d,p) (other atoms) basis set.

Table 4. Activation Energy Barriers, $\Delta E^{\ddagger}$, [in kcal/mol] for Hydroxylation and Epoxidation of Propene by $P450_{cam}$[a]

		$\Delta E^{\ddagger}$		
	profile	B3LYP-D2	B3LYP	B3LYP-D2//B3LYP
hydroxylation	1	11.9	14.8	12.2
	2	11.0	14.6	11.2
	3	13.6	17.0	15.6
	4	8.3	11.9	8.3
epoxidation	1	5.0	7.9	4.1
	2	8.2	13.2	8.9
	3	4.4	9.2	4.1
	4	8.3	11.5	6.0

[a]Barriers are calculated with QM/MM with (B3LYP-D2/CHARMM27 - B3LYP-D2) and without dispersion (B3LYP/CHARMM27 - B3LYP). Barriers are also calculated with B3LYP-D2/CHARMM27 at the B3LYP/CHARMM27 geometries (B3LYP-D2//B3LYP). The values presented in this table were calculated on the quartet spin surface with the LACV3P (Fe), 6-311++G(d,p) (other atoms) basis set.

hydroxylation profiles. This might not have been observed due the relatively low number of profiles sampled here. We have shown in previous work the importance of conformational sampling when using QM/MM calculations to predict selectivity.[20]

The B3LYP-D2 hydroxylation activation barriers span values ranging from 9.6 to 14.1 kcal/mol, and the epoxidation barriers span the range 10.3 to 14.8 kcal/mol. With zero point energy corrections (taken from previous gas-phase B3LYP calculations[34]), these ranges become 5.6 to 10.1 kcal/mol for hydroxylation and 9.7 to 14.2 kcal/mol for epoxidation. These values would predict a preference for hydroxylation, which is inconsistent with experiment, where roughly equal amounts of alcohol and epoxide are formed.[77,78] We again stress that this agreement would be expected to improve if more profiles were sampled and exact comparison with experiment is not the aim here. The main objective of the current work is to test the effect of the dispersion correction on barriers relative to those calculated without the correction, rather than to assess the ability of B3LYP-D2/MM to make predictions of selectivity. It is likely that both conformational sampling and dispersion effects should be included for the most reliable results.

Four profiles for the epoxidation and hydroxylation of propene were also calculated with and without the dispersion correction. The barriers are shown in Table 4. The B3LYP-D2 barriers barriers span the range 8.3 to 13.6 kcal/mol for hydroxylation and 4.4 to 8.3 kcal/mol for epoxidation. These barriers are significantly smaller than those calculated using B3LYP. With the barriers corrected for zero point energy, the B3LYP-D2 values span the range 4.8 to 10.1 kcal/mol for hydroxylation and 4.4 to 8.3 kcal/mol for epoxidation. This would suggest a slight preference for epoxidation over hydroxylation of propene during oxidation by $P450_{cam}$. While there are no experimental data for the oxidation of propene by this particular isoform, propene-1-oxide has been shown experimentally to be the only product observed during propene oxidation catalyzed by $P450_{LM2}$.[79] Again, full investigation of this preference by calculations would require extensive sampling, and the results here highlight also that inclusion of dispersion would be important too.

Regarding the effects of geometry optimization with dispersion, the difference between the B3LYP-D2//B3LYP and B3LYP-D2 barriers is smaller than that found for the larger substrates (camphor, cyclohexene, and benzene). In some cases, the B3LYP-D2//B3LYP barriers are the same as (or are smaller than) those calculated with B3LYP-D2. As propene has fewer atoms than cyclohexene, one would expect the dispersion correction to the propene barriers to be smaller than those calculated for cyclohexene. This is indeed found to be the case as the dispersion correction lowers the oxidation barriers by between 2.9 and 5.0 kcal/mol, compared to between 4.1 and 8.3 kcal/mol for cyclohexene oxidation.

Tests of Different Methods for Treatment of Dispersion. Grimme et al. recently reported an empirical dispersion correction (D3)[38] in which several refinements have been made over the original version used here (D2). Such refinements in D3 include the use of dispersion coefficients that are tailored to the specific nature and environment of the pair of atoms being considered, as well as the use of additional terms for higher-order moments (e.g., R^{-8} and R^{-10} terms). Most current implementations of the correction that are available in quantum chemical packages are based on the 2006 version (D2).[37] The magnitude of the correction obtained by the two versions was estimated by calculating the corrections to the barriers of hydrogen abstraction from camphor and both side-on and face-on addition of benzene to Cpd I with B3LYP-D2 and B3LYP-D3 (see Table 5). The geometries corresponding to the doublet reactant complexes and transition states from the B3LYP-D2/CHARMM27 calculations were used for these

Table 5. Dispersion Correction ΔE_{disp} [in kcal/mol] to B3LYP Barriers Calculated with B3LYP-D2[37] and B3LYP-D3[38] for Hydrogen Abstraction from Camphor by P450cam (CAM) and Side-on and Face-on Addition of Benzene to Cpd I of CYP2C9 (BEN-S and BEN-F Respectively)[a]

	ΔE_{disp}	
	B3LYP-D2	B3LYP-D3
CAM	−2.80	−1.80
BEN-S	−4.80	−3.21
BEN-F	−5.89	−3.53

[a]Corrections are calculated for geometries optimized at the B3LYP-D2/CHARMM27 level in the doublet spin state.

calculations. The dispersion correction is larger for the B3LYP-D2 calculated barriers, by as much as 2.4 kcal/mol (Table 5), with the largest difference observed between the barriers calculated for face-on benzene addition. It should be noted that the geometries used for this purpose were optimized using B3LYP-D2, and this may introduce a bias when considering B3LYP-D3 energy corrections. We are unable to optimize QM/MM geometries with B3LYP-D3 at present for technical reasons and hence cannot investigate any possible difference in geometry between the two methods. However, as the differences in geometry between the B3LYP and B3LYP-D2 QM/MM calculations are small, it is unlikely that there will be a significant difference between the B3LYP-D2 and B3LYP-D3 optimized geometries. Hence, if one assumes that the D2 correction overestimates the lowering of energy barriers, a pragmatic approach would be to use B3LYP-D3 single point calculations at the B3LYP-D2 calculated geometries.

In summary, the addition of an empirical dispersion correction is found to significantly lower the energy barriers to oxidation by Cpd I for all of the substrates studied here. The magnitude of this correction depends on both the size of the substrate and the orientation of the substrate relative to the heme. Addition of the empirical dispersion correction as a single point correction to the B3LYP calculated barriers (B3LYP-D2//B3LYP) results in a significant reduction in energy barrier. In most (but not all) cases, the barriers are reduced even more when structures are optimized with dispersion included. This observation is consistent with our previous QM-only study.[34]

Effects of Dispersion on Structures. As discussed in the Introduction, in our previous QM-only model study,[34] inclusion of a dispersion correction resulted in a significant change in the optimized geometries, for both the reactant complexes and the transition states. In all cases, the substrate molecule adopted a position closer to the heme moiety, such that the dispersion interaction was maximized. This was found for all the substrates studied. For the QM/MM calculations here, the difference between the geometries calculated with and without dispersion is small. While the substrate molecule is slightly closer to the heme when dispersion is included, this effect is far less pronounced than was observed in the gas phase calculations. The geometries of the QM/MM transition states for camphor hydroxylation, calculated with and without dispersion are superimposed in Figure 2. However, the effect on the geometry is more significant that one might expect merely from visual inspection of geometries. The inclusion of dispersion results in a slightly later transition state (with a shorter O−H distance) and the two reactants form an encounter complex geometry in which they are located closer together (Table 6). Additionally, the Fe−S bond length is found to be shorter in both the reactant complex and the transition state, with the dispersion correction found to have the largest effect on the latter species. A similar effect to that observed for camphor was observed for all of the other substrates studied here (details in the Supporting Information). This accounts for the change in barrier found when geometry optimization is performed.

It is apparent that the dispersion correction has a less pronounced (but not negligible) effect on the geometries optimized with QM/MM, compared to the analogous gas phase calculations. It is important to point out that the QM-only calculations are on smaller models. The smaller effect of dispersion on QM/MM geometries is due mostly to the restriction of the substrate orientation (relative to Cpd I) by the steric interactions of the surrounding protein and solvent environment. There is no fundamental difference between the QM parts of the QM/MM calculations here and our previous QM study,[34] except in the size of the model systems. While the effects of dispersion are small for optimization of structures, these are not insignificant for the calculation of barriers.

Many QM/MM studies of enzyme reactivity (including those presented here) will use a geometry sampled from a molecular dynamics simulation often carried out using a molecular mechanics forcefield for the starting structure(s). The forcefield will include a description of dispersion interactions between the atoms that will belong to the QM region in the QM/MM study. If the latter uses a QM method in which dispersion is not accounted for, QM/MM geometry optimization may therefore tend to lead to structures with larger nonbonded interatomic distances within the QM region. This will lead to a small but significant increase in the preferred volume occupied by the QM region in such QM/MM calculations. This may lead to artifacts in the calculations. Such problems will be removed by using a dispersion-corrected QM method in the QM/MM geometry optimization, which is inherently more consistent with MM forcefields. Finally, it is worthwhile to point out that correlated ab initio QM/MM calculations[29] will also be

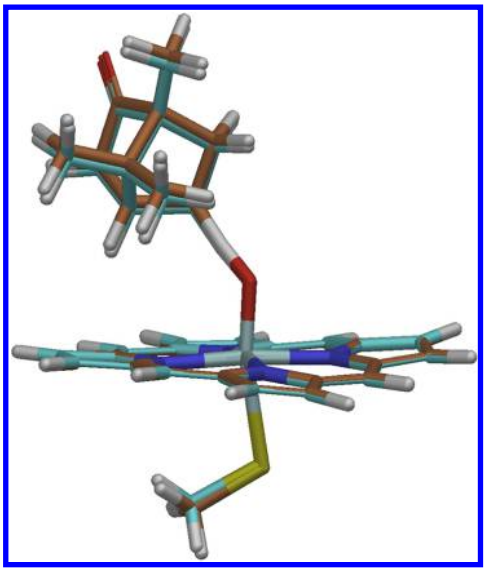

Figure 2. Superimposed geometries of the QM regions for the transition states for hydrogen abstraction from camphor by $P450_{cam}$, calculated at the B3LYP-D2/CHARMM27 (blue carbon atoms) and B3LYP/CHARMM27 (orange carbon atoms) levels.

Table 6. Fe−S, Fe−O, and O−H[a] Bond Lengths [in Å] for Calculated Geometries of Reactant Complexes (RC) and Transition States (TS) in the Hydrogen Abstraction of Camphor in $P450_{cam}$ with B3LYP-D2/CHARMM[b]

species	r(Fe−S)	r(Fe−O)	r(O−H)
^{2}RC	2.643 (2.663)	1.647 (1.649)	2.101 (2.349)
^{4}RC	2.643 (2.664)	1.643 (1.643)	2.101 (2.351)
^{2}TS	2.534 (2.671)	1.786 (1.780)	1.198 (1.201)
^{4}TS	2.510 (2.738)	1.774 (1.694)	1.197 (1.322)

[a]Where H is the 5-exo hydrogen of camphor. [b]Values corresponding to B3LYP/CHARMM calculated profiles are given in parentheses.

dx.doi.org/10.1021/ct300329h | J. Chem. Theory Comput. 2012, 8, 4637−4645

important for examining dispersion effects, but are not yet feasible for CYPs.

CONCLUDING REMARKS

Here we present a comprehensive study on the effect of an empirical dispersion correction on B3LYP-based QM/MM calculations of oxidation reactions catalyzed by $P450_{cam}$ and CYP2C9. The dispersion correction is found to lower energy barriers significantly, giving results in better agreement with experiment. For example, with dispersion included, the barrier to abstraction of hydrogen from camphor in $P450_{cam}$ is calculated to be lower than the upper limit suggested by experiment, whereas without dispersion the calculated energy barrier is too high. It is important to note that inclusion of the dispersion correction does not remove the need to sample multiple conformations,[20] but the work presented here suggests that dispersion should be included. The dispersion-corrected energy barriers are lower than those calculated without the correction, both when calculated for B3LYP/CHARMM27 and B3LYP-D2/CHARMM optimized geometries. The magnitude of the correction is greater in the latter case, and is also dependent on the orientation of the substrate relative to the heme and the size of the substrate. Similar effects are likely to be found with other DFT functionals that do not include dispersion, and indeed with other MM forcefields.

The effect of the dispersion correction on structures is much less pronounced than was observed in our previous QM-only study of small models.[34] However, this effect is sufficient to cause a notable lowering of the energy barriers; that is to say that optimization of geometries with dispersion results in a smaller change of structure than in QM calculations on small models. This is not surprising given the restraining effects of the MM environment in (larger) QM/MM models, as shown by the difference in energy between QM/MM geometries optimized with dispersion and those where the dispersion correction is applied as a single point correction. Additionally, since the QM-MM interaction energy calculated for B3LYP/CHARMM27 and B3LYP-D2/CHARMM27 calculations both include a dispersion contribution, the dispersion interaction is only missing for a small subset of atoms in the B3LYP/CHARMM27 calculations, relative to the size of the enzyme. However, the effect of the dispersion interaction on the geometry of the QM region is not negligible. As found in the QM-only study, the substrate and Cpd I in the dispersion-corrected optimized geometries are closer together in both the reactant complex and the transition state than those calculated without dispersion.

DFT methods that account for dispersion effects, such as the B3LYP-D2 method used here, have a very similar (or identical) computational cost to that of nondispersion corrected methods such as B3LYP. Given the significant effects of taking dispersion into account, we therefore strongly recommend that DFT-based QM/MM studies use dispersion-corrected QM methods, including for geometry optimization.

ASSOCIATED CONTENT

Supporting Information

QM, MM, and QM/MM energies are provided for all optimized structures, together with Mulliken charges, spin densities, and Cartesian coordinates of the QM regions. This material is available free of charge via the Internet at http://pubs.acs.org.

AUTHOR INFORMATION

Corresponding Author

*E-mail: jeremy.harvey@bristol.ac.uk (J.N.H.), adrian.mulholland@bristol.ac.uk (A.J.M.). Phone: +44 (0)117 954 6991. Fax: +44 (0)117 925 1295.

Notes

The authors declare no competing financial interest.

ACKNOWLEDGMENTS

A.J.M. is an EPSRC Leadership Fellow (Grant EP/G007705/01) and (together with R.L. and J.N.H.) thanks the EPSRC for support. A.J.M. and R.L. thank EPSRC for support under the CCP-BioSim project (Grant EP/J010588/1). We thank Prof. Stefan Grimme for providing the DFTD3 program.

REFERENCES

(1) Schöneboom, J. C.; Lin, H.; Reuter, N.; Thiel, W.; Cohen, S.; Ogliaro, F.; Shaik, S. *J. Am. Chem. Soc.* **2002**, *124*, 8142−8151.
(2) Lin, H.; Schöneboom, J.; Cohen, S.; Shaik, S.; Thiel, W. *J. Phys. Chem. B* **2004**, *108*, 10083−10088.
(3) Schöneboom, J. C.; Thiel, W. *J. Phys. Chem. B* **2004**, *108*, 7468−7478.
(4) Schöneboom, J. C.; Cohen, S.; Lin, H.; Shaik, S.; Thiel, W. *J. Am. Chem. Soc.* **2004**, *126*, 4017−4034.
(5) Bathelt, C. M.; Żurek, J.; Mulholland, A. J.; Harvey, J. N. *J. Am. Chem. Soc.* **2005**, *127*, 12900−12908.
(6) Altun, A.; Thiel, W. *J. Phys. Chem. B* **2005**, *109*, 1268−1280.
(7) Schöneboom, J. C.; Neese, F.; Thiel, W. *J. Am. Chem. Soc.* **2005**, *127*, 5840−5853.
(8) Harvey, J. N.; Bathelt, C. M.; Mulholland, A. J. *J. Comput. Chem.* **2006**, *27*, 1352−1362.
(9) Altun, A.; Shaik, S.; Thiel, W. *J. Comput. Chem.* **2006**, *27*, 1324−1337.
(10) Zheng, J.; Wang, D.; Thiel, W.; Shaik, S. *J. Am. Chem. Soc.* **2006**, *128*, 13204−13215.
(11) Altun, A.; Guallar, V.; Friesner, R. A.; Shaik, S.; Thiel, W. *J. Am. Chem. Soc.* **2006**, *128*, 3924−3925.
(12) Żurek, J.; Foloppe, N.; Harvey, J. N.; Mulholland, A. J. *Org. Biomol. Chem.* **2006**, *4*, 3931−3937.
(13) Altun, A.; Shaik, S.; Thiel, W. *J. Am. Chem. Soc.* **2007**, *129*, 8978−8987.
(14) Bathelt, C. M.; Mulholland, A. J.; Harvey, J. N. *J. Phys. Chem. A* **2008**, *112*, 13149−13156.
(15) Wang, D.; Zheng, J.; Shaik, S.; Thiel, W. *J. Phys. Chem. B* **2008**, *112*, 5126−5138.
(16) Altarsha, M.; Benighaus, T.; Kumar, D.; Thiel, W. *J. Am. Chem. Soc.* **2009**, *131*, 4755−4763.
(17) Wang, D.; Thiel, W. *J. Mol. Struct.: THEOCHEM* **2009**, *898*, 90−96.
(18) Altarsha, M.; Benighaus, T.; Kumar, D.; Thiel, W. *J. Biol. Inorg. Chem.* **2010**, *15*, 361−372.
(19) Shaik, S.; Cohen, S.; Wang, Y.; Chen, H.; Kumar, D.; Thiel, W. *Chem. Rev.* **2010**, *110*, 949−1017.
(20) Lonsdale, R.; Harvey, J. N.; Mulholland, A. J. *J. Phys. Chem. B* **2010**, *114*, 1156−62.
(21) Ranaghan, K. E.; Mulholland, A. J. *Int. Rev. Phys. Chem.* **2010**, *29*, 65−133.
(22) Olàh, J.; Mulholland, A. J.; Harvey, J. N. *Proc. Natl. Acad. Sci. U.S.A.* **2011**, *108*, 6050−6055.
(23) Lonsdale, R.; Olàh, J.; Mulholland, A. J.; Harvey, J. N. *J. Am. Chem. Soc.* **2011**, *133*, 15454−15474.
(24) Lonsdale, R.; Harvey, J. N.; Mulholland, A. J. In *Iron-Containing Enzymes: Versatile Catalysts of Hydroxylation Reactions in Nature.*; de Visser, S. P.; Kumar, D., Eds.; RSC Publishing: Cambridge, U.K., 2011; Chapter 11, pp 366−399.
(25) Lonsdale, R.; Harvey, J. N.; Mulholland, A. J. *Chem. Soc. Rev.* **2012**, *41*, 3025−3038.

(26) Guengerich, F. P. *Chem. Res. Toxicol.* **2001**, *14*, 611−650.
(27) Ogliaro, F.; Cohen, S.; de Visser, S. P.; Shaik, S. *J. Am. Chem. Soc.* **2000**, *122*, 12892−12893.
(28) Ogliaro, F. O.; de Visser, S. P.; Cohen, S.; Kaneti, J.; Shaik, S. *ChemBioChem* **2001**, *2*, 848.
(29) Claeyssens, F.; Harvey, J. N.; Manby, F. R.; Mata, R. A.; Mulholland, A. J.; Ranaghan, K. E.; Schütz, M.; Thiel, S.; Thiel, W.; Werner, H.-J. *Angew. Chem., Int. Ed.* **2006**, *45*, 6856−6859.
(30) Shaik, S.; Kumar, D.; de Visser, S. P.; Altun, A.; Thiel, W. *Chem. Rev.* **2005**, *105*, 2279−2328.
(31) van der Kamp, M. W.; Żurek, J.; Manby, F. R.; Harvey, J. N.; Mulholland, A. J. *J. Phys. Chem. B* **2010**, *114*, 11303−11314.
(32) Lonsdale, R.; Hoyle, S.; Grey, D. T.; Ridder, L.; Mulholland, A. J. *Biochemistry* **2012**, *51*, 1774−1786.
(33) Cohen, A. J.; Mori-Sánchez, P.; Yang, W. *Science* **2008**, *321*, 792−794.
(34) Lonsdale, R.; Harvey, J. N.; Mulholland, A. J. *J. Phys. Chem. Lett.* **2010**, *1*, 3232−3237.
(35) Johnson, E. R.; Mackie, I. D.; DiLabio, G. A. *J. Phys. Org. Chem.* **2009**, *22*, 1127−1135.
(36) Fey, N.; Ridgway, B. M.; Jover, J.; McMullin, C. L.; Harvey, J. N. *Dalton Trans.* **2011**, *40*, 11184−11191.
(37) Grimme, S. *J. Comput. Chem.* **2006**, *27*, 1787−1799.
(38) Grimme, S.; Antony, J.; Ehrlich, S.; Krieg, H. *J. Chem. Phys.* **2010**, *132*, 154104.
(39) Zhao, Y.; Truhlar, D. G. *Theor. Chem. Acc.* **2008**, *120*, 215−241.
(40) Becke, A. D.; Johnson, E. R. *J. Chem. Phys.* **2007**, *127*, 124108.
(41) Lai, W.; Chen, H.; Cohen, S.; Shaik, S. *J. Phys. Chem. Lett.* **2011**, *2*, 2229−2235.
(42) Schyman, P.; Lai, W.; Chen, H.; Wang, Y.; Shaik, S. *J. Am. Chem. Soc.* **2011**, *133*, 7977−7984.
(43) Tian, L.; Friesner, R. A. *J. Chem. Theory Comput.* **2009**, *5*, 1421−1431.
(44) Kast, P.; Asif-Ullah, M.; Hilvert, D. *Tetrahedron Lett.* **1996**, *37*, 2691−2694.
(45) Senn, H. M.; Käestner, J.; Breidung, J.; Thiel, W. *Can. J. Chem.* **2009**, *87*, 1322−1337.
(46) Ridder, L.; Mulholland, A. J.; Rietjens, I. M. C. M.; Vervoort, J. *J. Am. Chem. Soc.* **2000**, *122*, 8728−8738.
(47) Ridder, L.; Harvey, J. N.; Rietjens, I. M. C. M.; Vervoort, J.; Mulholland, A. J. *J. Phys. Chem. B* **2003**, *107*, 2118−2126.
(48) Bathelt, C. M.; Ridder, L.; Mulholland, A. J.; Harvey, J. N. *Org. Biomol. Chem.* **2004**, *2*, 2998−3005.
(49) Harvey, J. N. *Faraday Discuss.* **2004**, *127*, 165−177.
(50) *Jaguar*, 5th ed.; Schrödinger, LLC: Portland, OR, 2003.
(51) Vosko, S. H.; Wilk, L.; Nusair, M. *Can. J. Phys.* **1980**, *58*, 1200−1211.
(52) Becke, A. D. *J. Chem. Phys.* **1993**, *98*, 5648−5652.
(53) Stephens, P.; Devlin, F.; Chabalowski, C.; Frisch, M. *J. Phys. Chem.* **1994**, *98*, 11623−11627.
(54) Lee, C.; Yang, W.; Parr, R. *Phys. Rev. B* **1988**, *37*, 785−789.
(55) Hay, P.; Wadt, W. *J. Chem. Phys.* **1985**, *82*, 299−310.
(56) Rassolov, V.; Ratner, M.; Pople, J.; Redfern, P.; Curtiss, L. *J. Comput. Chem.* **2001**, *22*, 976−984.
(57) Hay, P. J.; Wadt, W. R. *J. Chem. Phys.* **1985**, *82*, 270−283.
(58) Clark, T.; Chandrasekhar, J.; Spitznagel, G. W.; Schleyer, P. V. R. *J. Comput. Chem.* **1983**, *4*, 294−301.
(59) Frisch, M. J.; Pople, J. A.; Binkley, J. S. *J. Chem. Phys.* **1984**, *80*, 3265−3269.
(60) McLean, A. D.; Chandler, G. S. *J. Chem. Phys.* **1980**, *72*, 5639−5648.
(61) Krishnan, R.; Binkley, J. S.; Seeger, R.; Pople, J. A. *J. Chem. Phys.* **1980**, *72*, 650−654.
(62) Ponder, J. W. *TINKER: Software Tools for Molecular Design*, 4th ed.; Department of Biochemistry and Molecular Biophysics, Washington University School of Medicine: Saint Louis, MO, 2003.
(63) Mackerell, A. D.; Bashford, D.; Bellott, M.; Dunbrack, R.; Evanseck, J.; Field, M.; Fischer, S.; Gao, J.; Guo, H.; Ha, S.; Joseph-McCarthy, D.; Kuchnir, L.; Kuczera, K.; Lau, F.; Mattos, C.; Michnick, S.; Ngo, T.; Nguyen, D.; Prodhom, B.; Reiher, W.; Roux, B.; Schlenkrich, M.; Smith, J.; Stote, R.; Straub, J.; Watanabe, M.; Wiorkiewicz-Kuczera, J.; Yin, D.; Karplus, M. *J. Phys. Chem. B* **1998**, *102*, 3586−3616.
(64) Singh, U. C.; Kollman, P. A. *J. Comput. Chem.* **1986**, *7*, 718−730.
(65) König, P. H.; Hoffmann, M.; Frauenheim, T.; Cui, Q. *J. Phys. Chem. B* **2005**, *109*, 9082−9095.
(66) (a) Bash, P. A.; Ho, L. L.; MacKerell, A. D.; Levine, D.; Hallstrom, P. *Proc. Natl. Acad. Sci. U.S.A.* **1996**, *93*, 3698−3703. (b) Freindorf, M.; Gao, J. *J. Comput. Chem.* **1996**, *17*, 386−395. (c) Freindorf, M.; Shao, Y.; Furlani, T. R.; Kong, J. *J. Comput. Chem.* **2005**, *26*, 1270−1278. (d) Luque, F. J.; Reuter, N.; Cartier, A.; Ruiz-López, M. F. *J. Phys. Chem. A* **2000**, *104*, 10923−10931. (e) Pentikäinen, U.; Shaw, K. E.; Senthilkumar, K.; Woods, C. J.; Mulholland, A. J. *J. Chem. Theor. Comput.* **2009**, *5*, 396−410. (f) Riccardi, D.; Li, G.; Cui, Q. *J. Phys. Chem. B* **2004**, *108*, 6467−6478.
(67) Grimme, S. *DFT-D3*, V2.1 Rev 6 ed.; University of Münster: Münster, Germany, 2011.
(68) Schlichting, I.; Berendzen, J.; Chu, K.; Stock, A. M.; Maves, S. A.; Benson, D. E.; Sweet, R. M.; Ringe, D.; Petsko, G. A.; Sligar, S. G. *Science* **2000**, *287*, 1615−1622.
(69) Williams, P. A.; Cosme, J.; Ward, A.; Angove, H. C.; Matak Vinkovic, D.; Jhoti, H. *Nature* **2003**, *424*, 464−468.
(70) Brooks, B. R.; Bruccoleri, R.; Olafson, B. D.; States, D. J.; Swaminathan, S.; Karplus, M. *J. Comput. Chem.* **1983**, *4*, 187−217.
(71) de Visser, S. P.; Ogliaro, F.; Sharma, P. K.; Shaik, S. *J. Am. Chem. Soc.* **2002**, *124*, 11809−11826.
(72) Bathelt, C. M.; Ridder, L.; Mulholland, A. J.; Harvey, J. N. *J. Am. Chem. Soc.* **2003**, *125*, 15004−15005.
(73) Filatov, M.; Harris, N.; Shaik, S. *Angew. Chem., Int. Ed.* **1999**, *38*, 3510−3512.
(74) Groves, J. T. *J. Chem. Educ.* **1985**, *62*, 928.
(75) Shaik, S.; Filatov, M.; Schröder, D.; Schwarz, H. *Chem.—Eur. J.* **1998**, *4*, 193−199.
(76) Rittle, J.; Green, M. T. *Science* **2010**, *330*, 933−937.
(77) White, R. E.; Groves, J. T.; McClusky, G. A. *Acta. Biol. Med. Ger.* **1979**, *38*, 475−482.
(78) Yoshioka, S.; Takahashi, S.; Ishimori, K.; Morishima, I. *J. Inorg. Biochem.* **2000**, *81*, 141−151.
(79) Groves, J. T.; Avarianeiser, G. E.; Fish, K. M.; Imachi, M.; Kuczkowski, R. L. *J. Am. Chem. Soc.* **1986**, *108*, 3837−3838.